비디오 현미경을 이용한 고분자 마이크로비드의 팽윤도 측정

조일훈 · 전승근* · 정현우* · 박상수*,†

을지대학교 임상병리학과, *을지대학교 의료공학과

(2023년 2월 7일 접수, 2023년 4월 28일 수정, 2023년 5월 2일 채택)

Swelling Ratio Determination of a Polymer Microbead *via* Video-Microscopy

Il-Hoon Cho, Seunggeun Jeon*, Hyun-Woo Jeong*, and Sangsoo Park*,†

Department of Biomedical Laboratory Science, Eulji University, Gyeonggi-do 13135, Korea
*Department of Biomedical Engineering, Eulji University, Gyeonggi-do 13135, Korea
(Received Februay 7, 2023; Revised April 28, 2023; Accepted May 2, 2023)

초록: 본 연구에서는 초흡수성 고분자 마이크로비드의 팽윤도를 측정하기 위한 비디오 현미경 이용법을 제안한다. 여성용 생리대에서 마이크로비드 입자를 분리하여 비디오 현미경 하에서 생리식염수를 첨가하였다. 마이크로비드의 팽윤 거동을 비디오로 녹화하고 이미지를 캡처하여 팽윤도 측정을 위한 마이크로비드의 투영면적을 계산하였다. 20개의 입자를 이용하여 투영면적으로 추정한 평형 상태에서의 팽윤도는 26.29(±3.11)로 기존 방법으로 구한 팽윤도 28.50(±1.25)보다 약 10% 작았다. 팽윤 거동의 비디오 현미경 관찰 및 마이크로비드의 팽윤도 측정은 위생용품 및 의료 제품에서 고흡수성 마이크로비드의 역할을 이해하기 위한 효과적인 방법이 될 수 있다.

Abstract: A simple video-microscopic method for measuring the swelling ratio of superabsorbent polymer (SAP) microbeads is suggested in this study. A microbead particle was isolated from a women's sanitary pad and was placed under a video-microscope, followed by the addition of buffered saline onto the microbead. The swelling behavior of the microbead was then videotaped and the images were captured to calculate the projected areas of the microbead for swelling ratio determination. Total of 20 microbeads were studied to measure the swelling ratio at equilibrium, and the ratio was 26.29 (±3.11), which was approximately 10% smaller than the swelling ratio determined by the conventional method, 28.50 (±1.25). Video-microscopic observation of the swelling behavior and estimation of the swelling ratio of SAP microbeads could become an effective tool for understanding the role of SAP microbeads in hygienic and medical products.

Keywords: superabsorbent polymer, superabsorbent microbead, hygienic products, medical products, swelling ratio, video-microscopic method.

Introduction

Superabsorbent polymers (SAPs) have been used in disposable diapers and feminine hygiene products, such as sanitary pads and tampons, mainly due to their high efficiency in absorbing body fluids, such as urine and menstrual discharge.[1-3] SAPs have also been applied in medical products for wound dressing, particularly for highly exuding wounds to handle excess exudate.[4-9] Polyacrylate-containing SAP particles in wound dressings are known to be particularly effective in the cleansing phase where the photolytic activity is high, which could result in tissue breakdown. As the water-absorbed SAPs behave as a hydrogel, the SAPs in wound dressings have also been called a superabsorbent hydrogel (SAH).

Traditionally, the absorbent cores of diapers and female hygienic products were made of cotton or cellulose fiber, but continuous efforts have been directed toward substituting it with SAPs.[1] The SAPs in hygienic products, mainly fabricated from acrylic acid and chemical cross-linkers, have a definite advantage compared with the cotton or cellulose fibers as they occupy a much smaller volume in a dry state. Furthermore, the cross-linked SAPs resist compression, after absorption of water, whereas the water-swelled cotton fibers are not cross-linked and thus are easily compressed by body weight when hydrated. Body fluid absorbed in cotton fibers is easily discharged when the swollen diaper or hygienic product is under

pressure by the body weight, resulting in leakage of absorbed urine or menstrual fluid and contamination of the skin around the absorbent products. In this way, the addition of SAPs in diapers and female hygienic products contributed greatly to the health of the users by reducing unwanted contact of bodily fluids with the skin.[3]

Recently, SAPs have been used as food for weight management purposes.[10-11] The SAP used in this purpose was carboxymethylcellulose cross-linked with citric acid, both of which are FDA-approved food grades. The dry SAP microparticles, 100-1000 μm, were enclosed in a capsule, and the capsules were taken with drinking water before a regular meal. Once they have reached the stomach, the capsules dissolve and the microparticles absorb water and swell to occupy the space inside the stomach. This causes an expansion of the stomach and stretching of the stomach muscles, which in turn activate the vagus nerve to trigger the signal for satiety and satiation.[10]

Optical microscopy is a powerful tool for investigating particles at the microscopic level. With this technique, it is possible to observe and characterize particles in a wide variety of polymeric materials and biological specimens including cells.[12-19] The objects in these studies however were either stationary with no morphological changes with time or quasi-stationary with the change occurring in long time scale. The swelling behavior of SAP is much faster, less than a minute in most cases, and is difficult to follow with conventional microscopy. In this report, we developed a videomicroscopic technique to monitor a fast-swelling behavior of an SAP and to estimate the swelling ratio of the particle, and compared the swelling ratio results with that obtained using a conventional method.

Although widely used in healthcare and medical applications, the in situ swelling behavior of SAPs has rarely been studied, as it is difficult to study because the SAP microbeads are mixed in the dispersed state with other constituents, and are difficult to isolate and collect enough amounts for swelling ratio determination. Instead most swelling studies of SAPs have been performed with bulk amount of SAPs in raw material state.[12,15-17] In short, the bulk mass of SAPs was measured before and after the absorption of water, and the swelling ratio was determined by the ratio of the SAP masses before and after swelling. In this report, we developed a videomicroscopic technique for estimation of an SAP swelling ratio, and compared the results with that obtained using a conventional method.

Experimental

Materials. A sanitary pad (Yejimiin; Yunseul Inc., Seoul, South Korea), the absorption core of which was composed of both cotton fibers and cross-linked polyacrylate microbeads, was obtained for the collection of SAP microbeads. The pad was cut open, and the absorption layer was separated from the other layers (Figure 1). The absorption layer was tapped above a 10 cm Petri dish using tweezers for SAP microbeads collection. A single SAP microbead was selected and transferred to a 5 cm Petri dish and placed under a video-microscope (ICS 305B; Sometech Inc., Seoul, South Korea) for observation. The main unit of the video-microscope provides an illuminating light through an optic cable to the microscope and digitizes the microscopic images from the 1/3 inch Sony CCDTM camera installed in the microscope and transmits the digital image data to a PC. The optic cable was positioned such that it can provide illumination from the side at approximately 45°. Microscopic images were taken at ×100 magnification. Total of 20 particles were studied for equilibrium swelling ratio measurement.

Several SAP microbeads collected were thoroughly dried and cut in half with a surgical blade under a stereo microscope, and they were placed on the stub of a scanning electron microscope (SEM) with sticky double-sided carbon tape. Platinum-coated samples were then examined using the field-emission SEM (S-4700; Hitachi, Japan).

Swelling Behavior Study. Copper sulfate pentahydrate (CuSO$_4$·5H$_2$O, 0.5 wt%; Showa, Japan) was added to a 0.1 M phosphate-buffered saline (PBS) solution (Sigma). Copper sulfate was added to visualize the SAP microbeads containing acrylate anions; Cu^{2+} ions are blue and easily adsorbed on the polyanions of the SAP microbeads. A single microbead was transferred onto a 5 cm Petri dish, which was placed under the video-microscope.
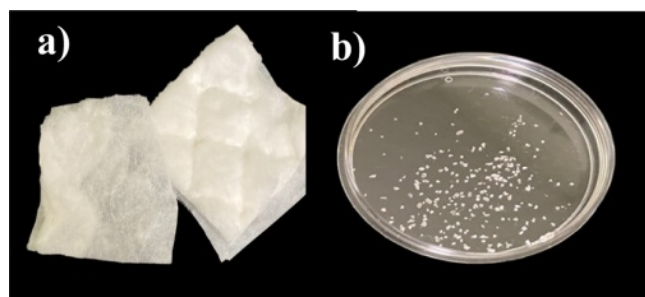

Figure 1. (a) Exposed absorption layer of a sanitary pad; (b) collected SAP microbeads from the pad.

A microscopic image of a dry microbead was obtained to calculate the projected area of the microbead in the dry state. Using a micropipette (Nichipet EX II; Nichiryo, Japan), a drop of $CuSO_4$-PBS solution was added to the microbead placed in a petri dish to estimate the area of the microbead image. Microscopic photographs were captured at predetermined intervals, and the projected areas of the blue SAP microbeads from their images were estimated using an image analysis program (IMT I-Solution, Vancouver, BC, Canada).

Estimation of Swelling Ratio. The swelling ratio of the SAP beads was obtained using the following equations. Both the SAP microbeads in the dry and hydrated states were assumed to be spherical, and the cut surface area in the middle of sphere A and volume of sphere V for a sphere with radius R is defined as follows:

$$A = \pi R^2 \ \text{ or } \ R = (A/\pi)^{1/2} \tag{1}$$
$$V = 4/3 \cdot \pi \cdot R^3 = 4/3 \cdot \pi^{-1/2} \cdot A^{3/2} \tag{2}$$

From eq. (2), the swelling ratio of the sphere at time t, $V(t)/V_0$, is defined as:

$$\text{Swelling ratio} = V(t)/V_0 = (A(t)/A_0)^{3/2} \tag{3}$$

where V_0 and $V(t)$ are the volumes of the SAP microbeads in the dry state and at time t after immersion in an aqueous environment.

Conventional Swelling Ratio Determination. Approximately 20 mg of SAP microbeads, collected from the sanitary pad, were allotted in each of four different 10 cm Petri dishes. The dishes were placed on a black background, and a ruler was placed under the dish for easy observation of the swelling behavior. The $CuSO_4$-PBS solution was then dropped onto the SAP microbeads until the beads were saturated. After 10 min, the remaining solution was removed by placing a water-absorbent Kintech wiper (Yuhan Kimberly, South Korea) onto the Petri dish. The dish was reweighed to calculate the mass of hydrated SAP beads. The swelling ratio was determined from the following equation, as suggested by Gulyuz[17]:

$$\text{Swelling ratio by mass} = (M_{eq}-M_0)/M_0 \tag{4}$$

where M_{eq} is the mass of the SAP microbeads in the equilibrium swollen state and M_0 in the dry state.

Results and Discussion

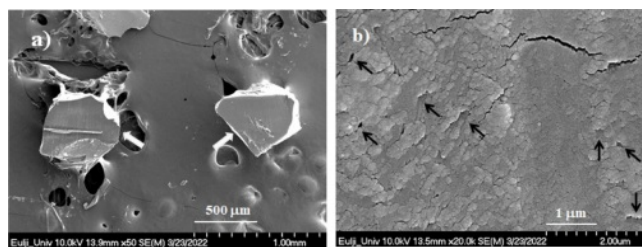**SEM and Videomicroscopic Images.** SEM images are shown in Figure 2. The cut surfaces of the SAP microbeads (a,

Figure 2. Scanning electron microscopic images of SAP particles obtained from a sanitary pad (a) at ×50; (b) at ×20000 magnification.

Table 1. Equilibrium Swelling Ratios Estimated by Video-microscopic Measurement

A_0, mm²	A_{eq}, mm²	V_{eq}/V_0
1.56	12.41	22.44
0.98	9.11	28.34
1.61	13.36	23.90
1.20	11.17	28.40
0.87	7.76	26.64
1.03	8.41	23.33
0.83	7.41	26.64
1.36	12.40	27.53
1.26	12.02	29.46
0.98	9.11	28.34
1.21	11.36	28.77
1.10	10.76	30.59
0.95	7.76	23.35
1.18	8.41	19.03
0.91	7.76	24.90
1.29	11.41	26.31
1.26	11.72	28.37
0.97	9.11	28.78
1.60	12.36	21.47
1.21	11.47	29.19
Average		= 26.29 (±3.11)

A_0: microbead area before swelling. A_{eq}: microbead area at equilibrium swelling. V_0: microbead volume before swelling. V_{eq}: microbead volume at equilibrium swelling. S.D.: standard deviation

white arrows) appeared clean and smooth at a magnification of ×50, except for artifacts in the cutting process. At a greater magnification of ×20000, the cut surfaces of the microbeads showed nanometer-scale cracks and voids (b, black arrows). The voids were believed to be the cracks perpendicular to the cut surface exposed by the cutting procedure.
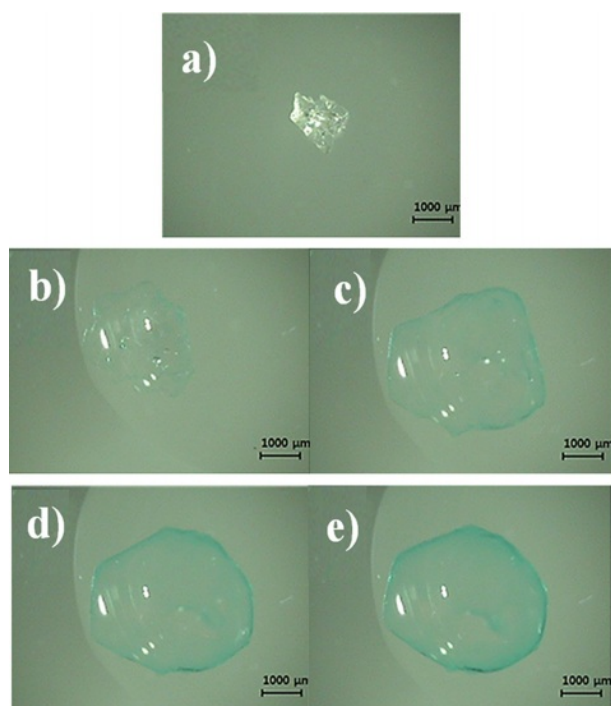
Figure 3. Video-microscopic images of an SAP microbead in a CuSO$_4$-PBS solution: dry state: (a) 10 s; (b) 50 s; (c) 120 s; (d) 240 s after immersion.
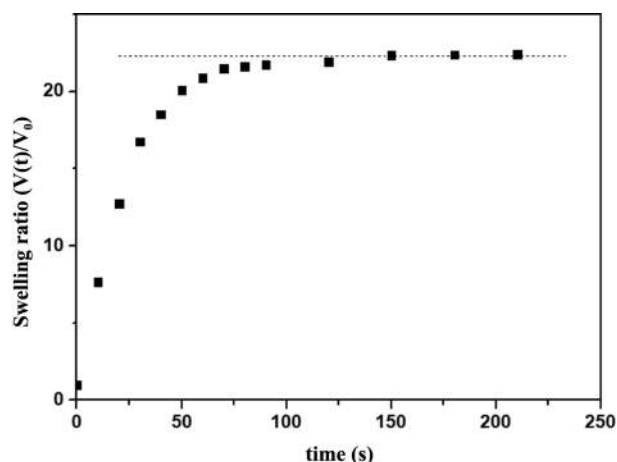

Figure 4. Swelling ratio of SAP microbeads after contact with CuSO$_4$-PBS solution. The dotted line was added to improve the visualization of the data points' position for the reader.

Table 2. Equilibrium Swelling Ratios as Determined by the Conventional Method

Lot #	M_0 (g)	M_{eq} (g)	M_{eq}/M_0
1	0.0210	0.6482	28.87
2	0.0215	0.6167	26.68
3	0.0207	0.6518	29.49
4	0.0208	0.6437	29.00
	Average		28.50 (±1.25)

Video-microscopic photographs of the SAP microbeads after the addition of CuSO$_4$-PBS are shown in Figure 3(a).

The original microbeads were transparent and irregular in shape. When a droplet of CuSO$_4$-PBS solution was added to the microbead, the microbead was enclosed by the droplet and expanded immediately, absorbing the aqueous milieu around it. The bright white spots in the hydrated SAP microbeads in Figure 3 are artifacts of light reflection. Within the first 10 s, the SAP bead swelled rapidly but the blue color around the bead was barely strong enough to identify the boundary of the bead (Figure 3(b)). At 50 s, the blue color at the circumference of the microbead became strong enough to easily identify the bead boundary. The color of the circumference of the microbeads clearly became more intense with time, but the microbeads did not swell any further after 120 s (Figures 3(d) and 3(e)). It should be noted that the circumference of the microbeads exhibited a darker blue color than the central space, indicating that the negatively charged segments of an SAP are not evenly distributed inside the hydrated SAP bead but are more localized around the surface of the bead.

Swelling Behavior. The swelling ratios of the microbeads at time t after contact with the CuSO$_4$-PBS solution were esti-

mated using eq. (3), and the results are shown in Figure 4. The swelling ratio increased rapidly with time up to 30 s but thereafter slowed down and reached an equilibrium value at approximately 2 min. The subsequent equilibrium swelling ratios calculated for twenty SAP microbeads are listed in Table 2. The initial area of the microbeads in the dry state ranged from 0.87 to 1.61 mm^2, and the equilibrium swelled area of SAP microbeads ranged from 7.41 to 12.41 mm^2. The estimated swelling ratio at equilibrium ranged from 19.03 to 30.59 with an average of 26.29 (±3.11).

Swelling Ratio by the Conventional Method. Photographs of the SAP microbeads before and after swelling in the CuSO$_4$-PBS solution are shown in Figure 5. The white SAP microbeads turned transparent blue upon absorption of the CuSO$_4$-PBS solution. The swelling ratios for four lots of SAP microbeads were calculated from the masses of the SAP microbeads in the dry state and those in the hydrated state, and the results are presented in Table 2. The average swelling ratio determined with four lots of SAP microbeads was 28.50 (± 1.25).
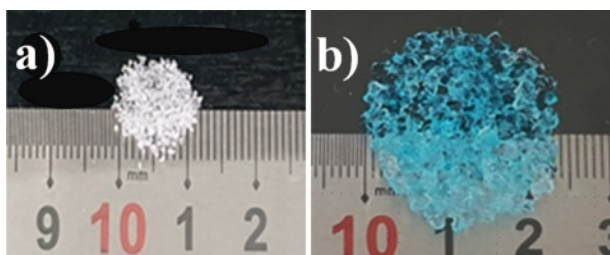
Figure 5. Photographs of (a) SAP microbeads collected for conventional swelling ratio determination; (b) the same microbeads equilibrated in a $CuSO_4$-PBS buffer.

The video-microscopic system for real-time observation of the SAP microbeads in this study was similar to that used by Maille *et al.*,[20] who studied the swelling behavior of a single coffee particle upon immersion in distilled water. Being black in color, the coffee particle was easily identifiable through light microscopy. However, the SAP microbeads in the present study were colorless in the hydrated state; thus, we dyed the microbeads with Cu^{2+} ions for easy identification through video-microscopy.

The microscopic size determination of SAP microbeads has seldom been reported in the literature.[15-17] Wu *et al.* prepared an SAP hydrogel with sodium alginate and chitosan solutions, and the SAP hydrogel was found to be spherical, but they did not attempt to measure the diameter or projected area of the hydrogel.[15] Instead, they employed the conventional method for swelling ratio determination by measuring the masses of the hydrogel in the dry and hydrated states. Fan *et al.* studied the pH dependence of a sunflower pollen hydrogel and measured the diameters of a spherical hydrogel in the optical micrographs and showed that the diameter of the gel increased from approximately 22 μm at pH 2 to approximately 42 μm at pH 10.[16] As they were only interested in the pH-dependent swelling/deswelling behavior of the pollen hydrogel, they did not attempt to measure the projected area of the pollen hydrogel. Guines *et al.* investigated the change in diameter of a cross-linked poly(aspartic acid) hydrogel upon addition of 1 M NaOH, which gives rise to carboxylate anions on the polymer backbone.[17] The measurement system comprised a microscope equipped with a polarized light lamp and a CCD camera. The diameters of the SAP hydrogels were measured from micrograph images. The SAP and pollen hydrogels in these studies were spherical, and we believe that the swelling ratio estimation of these hydrogels would have been possible.

Digital holographic microscopy (DHM), based on the principle of interference between a reference beam and a scattered light field from the sample, is a new optical microscopy technique that allows for visualization of living cells with high temporal and spatial resolution. This technique was very successful for investigating the effect of osmotic pressure on RBC shape or the effect of blood flow on RBC deformability, as well as to assess the spherical deformation of HeLa cancer cells induced by trypsin treatment.[18-19] However, application of DHM technique to this SAP microbead system would have been difficult since the DHM is a more complicated system with many components including laser, mirrors and beam splitters. In the study of HeLa cancer cell deformation, the authors reported that they needed 5 min after adding trypsin to adjust the observation conditions.[19] We believe that DHM is more appropriate for the shape changes occurring in a time scale of tens of minutes.

We note that the effect of the ionic strength of the solution on the swelling behavior of the SAP microbead has not been investigated in this study. The concentration of the copper sulfate in the experimental solution, 0.5 wt% $CuSO_4$ in 0.1 M Phosphate buffer at pH 7.4, is calculated to be 0.2 M and ionic strength contribution of the copper sulfate is 0.8 M. The ionic strength of the PBS is calculated to be 0.163 M.[20] The combined ionic strength of the experimental solution was thus 0.963 M. Although the ionic strength of the solution is rather high, it is still in the good solvent condition, as evidenced by fast swelling of the SAP microbead in Figure 3. While trying to investigate the swelling behavior at a lower ionic strength, we encountered with two problems. The first problem was lightness of the color of the swelled SAP microbead, particularly at the early stage of swelling in which Cu^{2+} ion inside the swelled polyelectrolyte is too low and the green color of the boundary of the SAP microbead was barely discernable, as can be expected from the result in Figure 3(b). The second problem was too fast a swelling of the SAP particle at low ionic strength; the microbead swelled almost instantly when distilled water was added instead of the $CuSO_4$-PBS solution, and it was difficult to adjust the observation conditions such as spatial arrangement of the sample and focusing of the lens in time to monitor the swelling behavior. We believe that this videomicroscopic technique is appropriate for monitoring deformation of the particle that takes more than 10 seconds.

There are several methods of conventional swelling ratio determination for SAP microbead/hydrogel materials, including the tea-bag, sieve, and filtration methods. However, each method has serious systematic drawbacks, as has been well

documented by Zhang *et al.*[21] In brief, there are problems related to whether free swelling is possible for the particles, the difference in techniques for removing excess liquid, and the effect of water absorbed by the container. There is no well-established standard protocol for conventional methods, and their reproducibility is not high among institutions using the same protocol.[22] With this background information in mind, we note that there is only a 10% difference in swelling ratios between the video-microscopic values and those determined by the conventional method, as shown in Tables 1, 2. We believe there are two main reasons for this discrepancy. First, the microbeads in the dry state were not completely spherical, as observed in the micrographs (Figures 2, 3). Thus, the volume estimation using Equation 2 might have been inaccurate. As the microbeads tended to lie flat on the bottom of the Petri dish with as much contact area as possible, we suspect that there could have been an overestimation of the microbead volume when the volume was estimated from the projection area of a non-spherical microbead. Second, we suspect that the nanoporous nature of the SAP microbeads contributed to the smaller swelling ratio estimated from the projected area ratio because the nanoporous voids inside an SAP microbead contribute to the volume of the microbead but not its mass.[23-26]

Conclusions

We isolated SAP microbeads from a sanitary pad and measured the projected areas of the beads in the dry and swollen states using video-microscopic images. The swelling ratios were estimated from the projected areas of the microbeads, assuming that the dry microbeads had a spherical shape. The swelling ratios estimated in this study had a 10% difference from those measured by the conventional method.

Copper sulfate was useful for visualizing the SAP beads that are colorless after hydration and may be an effective visualization tool for observing anionic SAPs in the hydrated state by microscopy. The study of SAP microbead swelling behavior by video-microscopy has advantages over the conventional swelling ratio determination method; the in situ behavior of the SAP microbeads and hydrogels in real time could be investigated, and the process does not require a large sample size. Thus, this technique could be a useful tool for investigating the swelling behavior of SAP microbeads and hydrogels and warrants further studies to become an established method for swelling ratio determination.

Conflict of Interest: The authors declare that there is no conflict of interest.

References

1. Kosemund K.; Schlatter H.; Ochsenhirt J. L.; Krause, E. L.; Marsman, D. S.; Erasala, G. N. Safety evaluation of superabsorbent baby diapers. *Regul Toxicol Pharmacol* **2009**, 53, 81-89.

2. Magnay, J. L.; Nevatte, T. M.; Dhingra, V.; O'Brien, S. Menstrual Blood Loss Measurement: Validation of the Alkaline Hematin Technique for Feminine Hygiene Products Containing Superabsorbent Polymers. *Fertil Steril* **2010**, 94, 2742-2746.

3. Runeman, B. Skin Interaction with Absorbent Hygiene Products. *Clin Dermatol* **2008**, 26, 45-51.

4. Wiegand, C.; Abel, M.; Ruth, P.; Hipler, U. C. Superabsorbent Polymer-containing Wound Dressings Have a Beneficial Effect on Wound Healing by Reducing PMN Elastase Concentration and Inhibiting Microbial Growth. *J. Mater. Sci. Mater. Med.* **2011**, 22, 2583-2590.

5. Kumar, S. K. S.; Prakash, C.; Vaidheeswaran, S.; Kumar, B. K.; Subramanian, S. Design and Characterization of Secondary and Tertiary Layers of a Multilayer Wound Dressing System. *J. Test. Eval.* **2018**, 48, 2683-2698.

6. Barrett, S.; Callaghan, R.; Chadwick, P.; Haycocks, S.; Rippon, M.; Stephen-Haynes, J.; Simm, S. An Observational Study of a Superabsorbent Polymer Dressing Evaluated by Clinicians and Patients. *J. Wound. Care.* **2018**, 27, 91-100.

7. Barrett, S.; Welch, D.; Rippon, M. G.; Rogers, A. A. Clinical Evaluation of a Superabsorbent Polymer Dressing in Enabling Self-care of Wounds. *Br J. Commun. Nurs.* **2020**, 25, Suppl 6, S28-S36.

8. Sharp, C. Managing the Wound with Hydration Response® Technology. *Wounds UK* **2010**, 6, 112-115.

9. Browning, P.; White, R. J.; Rowell, T. Comparative Evaluation of the Functional Properties of Superabsorbent Dressings and Their Effect on Exudate Management. *J. Wound. Care.* **2016**, 25, 452-462.

10. Aronne, L. J.; Anderson, J. E.; Sannino, A.; Chiquette, E. Recent Advances in Therapies Utilizing Superabsorbent Hydrogel Technology for Weight Management: a Review. *Obes Sci Pract.*

11. Giruzzi, N. Plenity (oral superabsorbent hydrogel). *Clin Diabetes* **2020**, 38, 313-314.

12. Sanaei Moghaddam Sabzevar Z.; Mehrshad, M.; Naimipour, M. A Biological Magnetic Nano-hydrogel Based On Basil Seed Mucilage: Study of Swelling Ratio and Drug Delivery. *Iran. Polym.* **2021**, 30, 485-493.

13. Duncanson, W. J.; Lin, T.; Abate, A. R.; Seiffert, S.; Shah, R. K.; Weitz, D. A. Microfluidic Synthesis of Advanced Microparticles

for Encapsulation and Controlled Release. *Lab. on a Chip.* **2012**, 12, 2135-2145.

14. Liu, S.; Deng, R.; Li, W.; Zhu, J. Polymer Microparticles with Controllable Surface Textures Generated Through Interfacial Instabilities of Emulsion Droplets. *Adv. Func. Mater.* **2012**, 22, 1692-1697.

15. Wu, T.; Huang, J.; Jiang, Y.; Hu, Y.; Ye, X.; Liu, D.; Chen, J. Formation of Hydrogels Based on Chitosan/alginate for the Delivery of Lysozyme and Their Antibacterial Activity. *Food Chem* **2018**, 240, 361-369.

16. Fan, T. F.; Hwang, Y.; Ibrahim, M. S.; Ferracci, G.; Cho, N. J. Influence of Chemical and Physical Change of Pollen Microgels on Swelling/de-swelling Behavior. *Macromol. Rapid Commun.* **2020**, 41, e2000155.

17. Gyenes, T.; Torma, V.; Zrínyi, M. Swelling Properties of Aspartic Acid-based Hydrogels. *Colloids Surf A Physicochem Eng Aspects* **2008**, 319, 154-158.

18. Memmolo, P.; Miccio, L.; Merola, F.; Ferraro, P. The Talbot Effect in Self-assembled Red Blood Cells Investigated by Digital Holography. *J. Physics: Photonics* **2020**, 2, 035005.

19. Yamazaki, T.; Hirayama, K.; Matsukawa, Y.; Takemura, M.; Umemura, K. Digital Holographic Microscopy of Living Hela Cells Before and After Enzyme Treatments. *In Proceedings of the 6th International Conference on Biomedical Engineering and Applications*, Hangzhou, China, May 13-15, 2022; pp 127-129.

20. Moon, M. H.; Park, I.; Kim, Y. Size Characterization of Liposomes by Flow Field-flow Fractionation and Photon Correlation Spectroscopy: Effect of Ionic Strength and pH of Carrier Solutions.

J. Chromatography A, **1998**, 813, 91-100.

21. Maille, M. J.; Sala, K.; Scott, D. M.; Zukswert, H. Critical Examination of Particle Swelling During Wetting of Ground Coffee. *J. Food. Eng.* **2021**, 295, 110420.

22. Zhang, K.; Feng, W.; Jin, C. Protocol Efficiently Measuring the Swelling Rate of Hydrogels. *MethodsX* **2020**, 7, 100779.

23. Mechtcherine, V.; Snoeck, D.; Schröfl, C.; De Belie, N.; Klemm, A. J.; Ichimiya, K. Falikman, V. Testing Superabsorbent Polymer (SAP) Sorption Properties Prior to Implementation in Concrete: Results of a RILEM Round-robin Test. *Mater. Struct.* **2018**, 51, 28.

24. Wang, W.; Zong, L.; Wang, A. A Nanoporous Hydrogel Based on Vinyl-functionalized Alginate for Efficient Absorption and Removal of Pb^{2+} ions. *Int. J. Biol. Macromol.* **2013**, 62, 225-231.

25. Kumar, B.; Priyadarshi, R.; Sauraj, Deeba, F.; Kulshreshtha, A.; Gaikwad, K. K.; Negi, Y. S. Nanoporous Sodium Carboxymethyl Cellulose-g-poly (sodium acrylate)/fecl₃ Hydrogel Beads: Synthesis and Characterization. *Gels* **2020**, 6, 49.

26. Soleyman, R.; Rezanejade, B. G.; Pourjavadi, A.; Varamesh, A.; Davoodi, A. A. Hydrolyzed Salep/gelatin-g-polyacrylamide as a Novel Micro/nano-porous Superabsorbent Hydrogel: Synthesis; Optimization and Investigation on Swelling Behavior. *Sci. Iran.* **2015**, 22, 883-893.